Numerical simulation of deformations of a specimen of a composite helicopter blade as part of a resonant vibration set-up

D. Fedorov[1] and *K.* Shcherban[1*]

[1]TsAGI, Zhukovsky, Moscow region, Russia, «Strela» branch of MAI, Zhukovsky, Moscow region, Russia

Abstract. To determine the fatigue life of the tail rotor blade of a helicopter made of polymer composite materials (CM), a method of fatigue testing of the specimens of the blade with accompanied numerical modeling of the deformed state has been developed. The tests are carried out on a resonant vibration set-up, with simultaneous reproduction of a forcing harmonic transverse force and a constant longitudinal tensile force. The tests are carried out by a vibration loading mode equivalent in fatigue damage, which includes one level of variable load in the thrust plane and in the plane of rotation. The equivalent mode is formed based on the variable loading spectrum of the blade, which is obtained from the results of flight measurements of the loads on the tail rotor, as well as the repeatability of the expected operating conditions of the helicopter. The tests are accompanied by computational and experimental studies, which include finite element calculation of the stress state and modal analysis of the standard blade and the test specimen, as well as the strain measuring of the structure. According to the results of the research, the vibration loading modes are corrected.

1 Introduction

In both domestic and foreign practice, the determining role in testing the durability of tail rotor blades is assigned to fatigue tests of full-scale structure [1-2]. Such tests make it possible to choose rational variants of the blade structure, determine their durability and recommend them for expanded production, ensuring their certification. In operation, the blade is subjected to a complex of variable aerodynamic and inertial loads that cause axial tensioning of the blade, as well as its bending in the planes of thrust and rotation. Fatigue tests of a full-scale blade with cyclic loading with an operational spectrum are practically impossible, due to the unacceptable duration of such tests, as well as due to technical difficulties in reproducing it. In order to reduce the duration of laboratory tests and simplify them in tests, the operational load spectrum is replaced by an equivalent regime, which introduces the same fatigue damage to the blade structure as the operational spectrum [3-4]. Fatigue tests of helicopter blades, as a rule, are carried out under the simultaneous action of a forcing harmonic transverse force and a constant longitudinal tensile force in resonant vibration set-

* Corresponding author: kscherban@mail.ru

up [5-12]. In such vibration set-up, an eccentric vibrator with an electric drive is used to excite the vibrations of the blade, and a mechanical device is used to create a tensile force. Finite element modeling of blade loading in set-up conditions and operation allows us to confirm the adequacy of test modes and operating conditions [13].

The purpose of this article is numerical simulation of deformations of a specimen of a composite helicopter blade as part of a resonant vibration set-up.

2 Method of fatigue testing of blade specimen

For the purpose of full-scale simulation of the structure of the blade, a specimen was made from a tail rotor blade maded according to production technology. Its structure included the main sections of the full-scale blade (root part (RP), a transition (TP) and part (RgP) of the regular one) (2), as well as a steel junction node (1) for connecting the blades and two steel plates (3) for applying axial force (fig. 1).

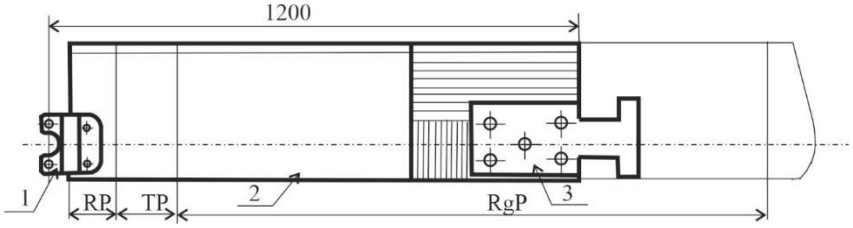

Fig. 1. Test specimen.

The end part of the regular section was reinforced, and two steel plates were attached to it to apply axial force. In cross-section, the transitional and regular sections represented a closed aerodynamic profile consisting of a spar and a tail section.

Fatigue tests were carried out by an equivalent mode, which was formed based on the spectrum of variable loads, which was obtained from the results of flight measurements of the loads on the tail rotor and the repeatability of modes per flight for the helicopter. In each mode, the bending moments in the thrust plane and in the plane of rotation in the characteristic sections of the rotor blade are measured. The realizations of bending moments are systematized by the method of full cycles and by the linear summation hypothesis, the amplitudes of symmetric equivalent cycles at each of the flight modes are determined. According to the integral repeatability in the control sections, the amplitudes of symmetric cycles are determined, which have equivalent damage. The obtained distribution of amplitudes of equivalent moments in characteristic cross sections is reproduced on a resonant set-up (fig.

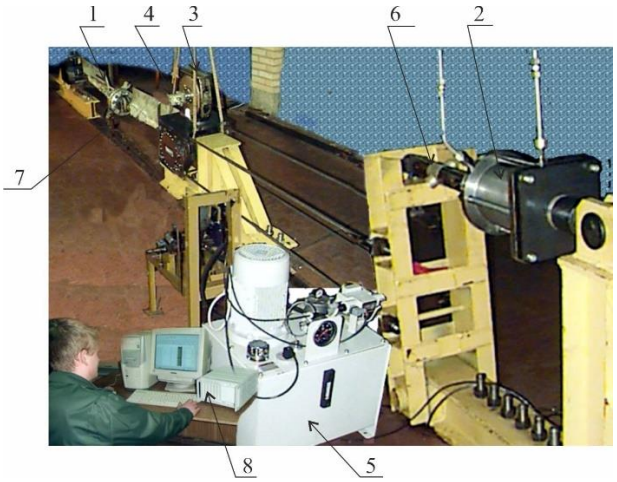

Fig. 2. Full-scale fatigue test resonant set-up.

The specimen was loaded with axial force using a hydraulic cylinder (2). The bending vibrations of the blades were excited by a two-block (eccentric) inertial vibrator (3) mounted on one of the blades. To rotate the vibrator, a hydraulic motor (4) was used, mounted on a support and connected to the vibrator using a flexible roller. An oil pumping station (5) powered the hydraulic cylinder and the hydraulic motor. A dynamometer (6) was used to measuring the specified axial force acting on the blade specimen. The vibration-loading mode, i.e. the amplitude and frequency of vibrations, was maintained using a displacement sensor (7) and an automatic control system (8). During reproducing static and vibration loading, a strain measuring in control sections was made (Fig. 3).

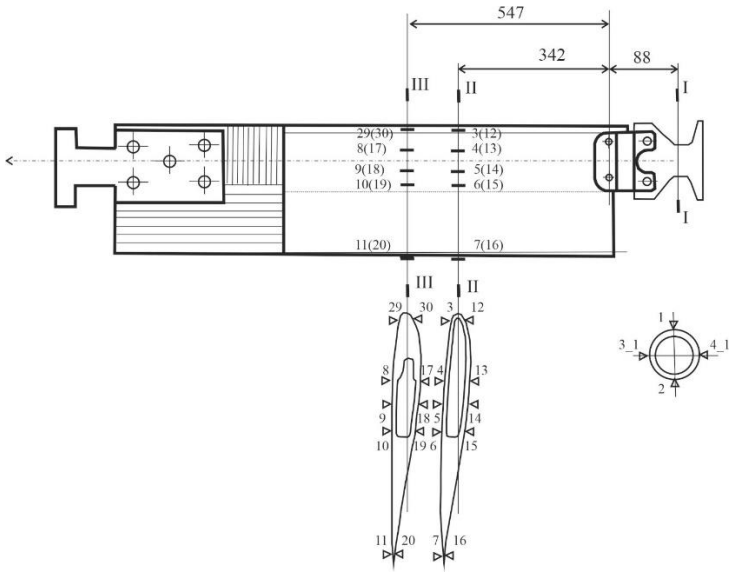

Fig. 3. Scheme of strain gages.

3 Finite element simulation of blade loading

For the computational support of the tests, finite element (CE) models of the blade (fig. 4a) and of the specimen consisting of two sections of blades joined by root (Fig. 4b) were developed. The structure simulation and calculations were carried out based on the NASTRAN system [14].

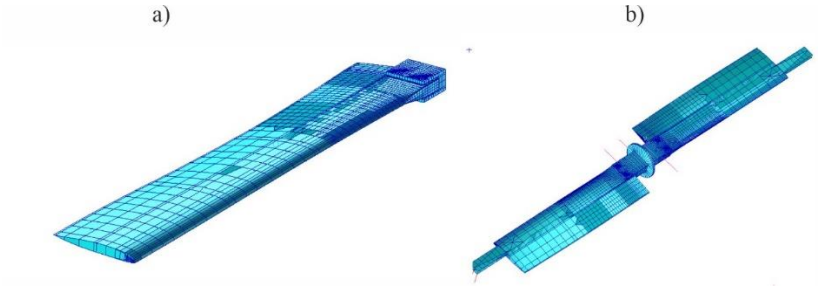

Fig. 4. Finite element models: a) the blade, b) the specimen.

The CE model of the blade (Fig. 4a) reflected the main structural elements, namely: a spar, a tailpiece, a tip, an anti-flutter load, a rubber anti-erosion layer, fetter (a metal overlay on the rubber layer), an end fairing. Modeling of the shells of the spar and the bearing layers of the shank was carried out using quadrangular and triangular shell elements formed based on a composite material. In addition, shell finite elements were used to model the shackle. Spatial three-dimensional finite elements in the form of hexahedra and triangular prisms were used to model structural elements made of "chopped" fiberglass, rubber, textolite, honeycomb filler of the shank, as well as tips and bolts. Modeling of a wire anti-flutter load was carried out using rod finite elements. Since the main rigidity of the blade structure was contained in the spar, its model was built based on quadrangular elements (only in the transition zone to a rarer grid, several triangular elements were used). Actually, the tip is not of interest from the point of view of determining its stress-strain state. For this reason, it was modeled approximately, but with mass retention, using hexahedral elements, and bolts with elements in the form of triangular prisms. Of course, the element model of the blade included 6300 nodes and about 30,000 variables. To model composite materials in all sections, the spar and bearing layers of the shank were formed based on a single type monolayer made of fiberglass T60. The number of monolayers and their laying varied, depending on the location.

During the simulation, the masses of all known structural elements were determined, and their comparison with the masses of the corresponding finite elements was carried out in order to correct the latter if necessary. This correction was very insignificant in all cases. This made it possible to accurately determine the structural masses of the sections, and therefore the mass summary of the finite element model of the blade structure seems quite satisfactory.

The CE model of the specimen is shown in figure 4b. The following modifications were made with each of the blades:

- the length was reduced;
- a connecting disc with a fork was introduced between the two specimen of blades to connect the specimens by the root parts;
- steel plates were attached to the specimens in the tip to transfer axial force.

4 Discussion of research results

4.1 Modal analysis of the blade

For experimental confirmation of the correctness of finite element modeling of the blade, the calculation of the own shapers and frequencies of a non-rotating blade with rigid attachment according to a cantilever scheme was carry-outed and a comparison with the experimental results was performed. The results for the three lowest frequencies and the deviation of the calculation from the experiment ε (%) are shown in table 1.

Table 1. Own shapers and frequencies of blade.

№	Frequencies (Hz)		ε (%)	Description of the tone
	Calculation	Experiment		
1	6.52	7.0	-6.86	1st bend in the thrust plane
2	34.67	33.0	+5.06	1st bend in the plane of rotation
3	74.91	70.0	+7.01	Torsion

The comparison shows satisfactory convergence of the calculation with the experiment, which made it possible to use the developed CE model for subsequent analysis. Figure 5 shows the images of the oscillation forms obtained by calculation, together with the image of an undeformed structure.

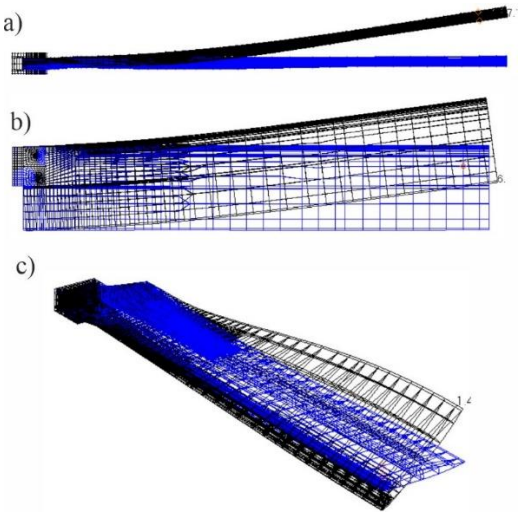

Fig. 5. Own shapes of blade oscillation: a) 1st bend in the thrust plane, b) 1st bend in the plane of rotation, c) torsion.

4.2 Investigation of deformations and deflections of the specimen

Deformations are the only quantity that has a physical meaning, and admitting the same interpretation in this case, both in the case of experiment and in the case of calculation. Therefore, to compare the results of the calculation and experiment, a study of deformations for both static and dynamic loading of the sample was performed.

Three cases of static loading of the sample were considered:

- axial tension;
- transverse bending in the thrust plane;
- transverse bending in the plane of rotation.

A vertical force applied in the end section of the specimen created the transverse bending loading. The values of the transverse forces were determined from the conditions so that the bending moment in the section I-I during bending in the thrust plane and in the plane of rotation reached the specified values. The specimen was fixed according to the cantilever scheme in the root section. The longitudinal force applied to the specimen created the axial loading. The results of strain measurements and calculation under static loading of the specimen by axial force, as well as by the transverse force in the planes of thrust and rotation are shown in figure 6. From the consideration of the figure, it can be noted that the results of deformation measurements and calculation under static loading of the specimen, both by axial force and transverse bending, are satisfactory.

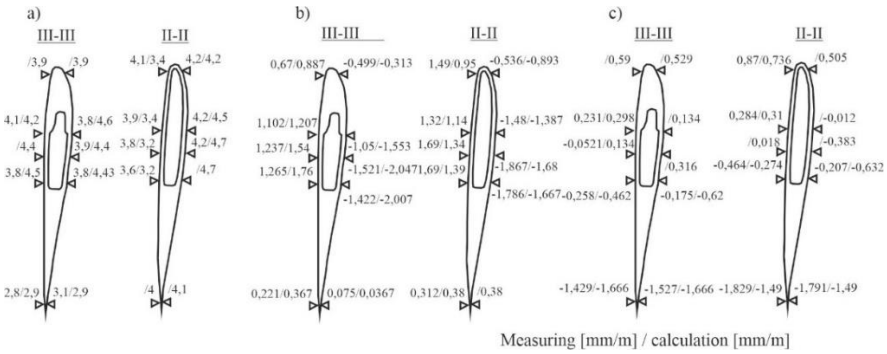

Fig. 6. Deformation in cross section of blade under loading by: a) axial force, b) transverse force in the planes of thrust, c) transverse force in the planes of rotation.

The excitation of oscillations in the thrust plane and in the plane of rotation with the preliminary application of an axial tensile load was considered during the dynamic loading of the blade specimen. The amplitude of the oscillations of the excitation force (or displacement) is unknown, and their determination is a complex nonlinear task. This task can be simplified by solving it by introducing an elastic support at the end of the blade into the model. The stiffness of this support is an unknown quantity. In this case, calculations were carried out in which the stiffness of the support was as a parameter. The calculated and experimental amplitudes of deflections under the force exciting the oscillations were compared. The distributions of deflection amplitudes obtained by calculation and measurements of the specimen when oscillations are excited under set-up conditions are shown in figure 7.

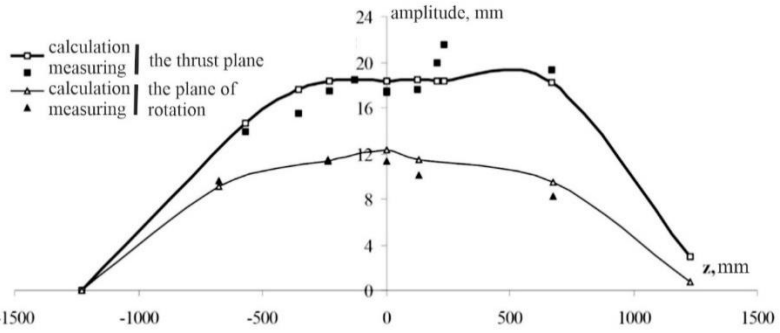

Fig. 7. Distributions of deflection amplitudes along the length of the blade specimen.

In the set-up conditions, the oscillation forms of the specimen are shown in figure 8. The frequency of oscillations in the thrust plane obtained by calculation was 10,9 Hz, and the measured was 11 Hz. The frequency of oscillations in the plane of rotation obtained by calculation (17,3 Hz) also slightly differed from the measured frequency (17 Hz).

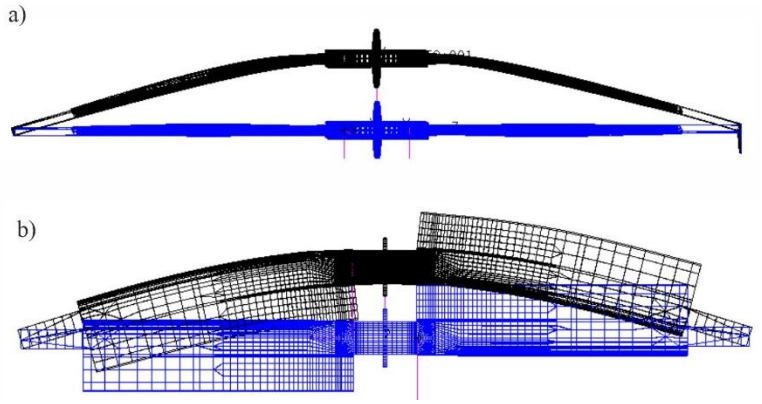

Fig. 8. Shapes of blade oscillation: a) bend in the thrust plane, б) bend in the plane of rotation.

The amplitudes of deformations obtained by measuring and calculation during excitation of vibrations in the plane of thrust and rotation are shown in figure 9.

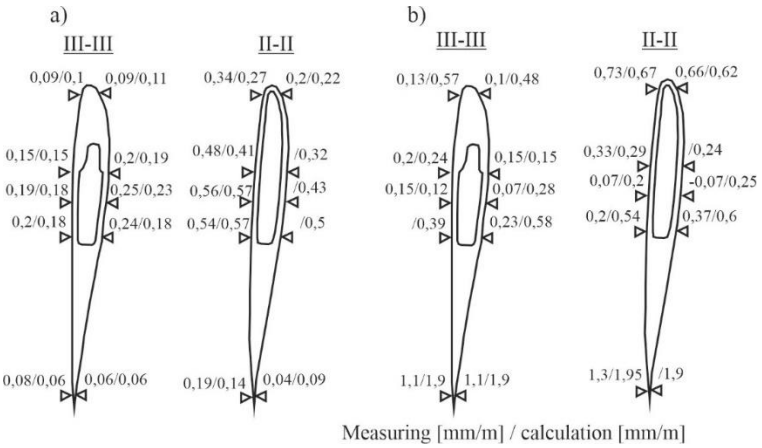

Fig. 9. The amplitudes of deformations during excitation of vibrations: a) in the plane of thrust, b) in the plane of rotation.

Comparison of the vibration amplitudes of deformations obtained by calculation and strain measurement shows their satisfactory convergence. The amplitudes of deformation cycles and deformations obtained by static strain measurement allowed us to correct the amplitudes of bending moment cycles in control sections.

5 Conclusion

The developed finite element model of the composite blade reflects the main stiffness and mass characteristics of the structure. This is confirmed by comparing the own shapes and frequencies obtained by calculation and experiment. The frequency deviation does not exceed 7%.

Finite element modeling of a specimen of two blades joined together as part of a resonant set-up makes it possible to determine deflections and deformations of the specimen under vibration loading. The correctness of the finite element modeling of the blade is confirmed by comparing the deflections and deformations obtained by calculation and measurements under vibration loading.

References

1. J.K. Tadich, J. Wedel-Heinen, Proceedings of EMEC **63**, 1-10 (2007)
2. B. Rusuo, Proceedings of ICAS, 1-4 (2010)
3. G. Freebury, W. Musial, Determining equivalent damage loading for full-scale wind turbine blade fatigue tests, AIAA **0060** (2000)
4. A. Jayantha, l. Epaarachchi, D. Philip Clausen, International Conference SIF «Structural Integrity and Fracture», 111- 118 (2004)
5. L.N. Yakimenko, Proceedings of TsAGI **2642**, 51-54 (2001)
6. L.N. Ekimenkov, Tests of helicopter blade units Aviation industry **6**, 72-73 (1963)
7. Yu.Ya. Betkovsky, G.A. Vershinin, V.T. Bustard, A.F. Makarov, *Method of testing cantilever structures for endurance under dynamic loading patent RU 2 301 413 C1 (2007)*
8. F.X. Netfullov, V.V. Ogorodov, V.A. Shuvalov, A. Dvoryankin, *Method of dynamic testing of helicopter tail rotor blades for fatigue strength patent RU 2 196 313 C2 (2003)*
9. P.S. Shelkovnikov, *Dynamic test set-up of aircraft propeller elements patent RU 2 102 713 C1* (1998)
10. B.S. Sirotinsky, F.H. Netfullov, V.M. Pchelkin, N.I. Doroshenko, *Fatigue test set-up for aircraft propeller blades specimen patent RU 2 163 714 C1* (2001)
11. N.I. Goryachev, L.N. Yakimenko, S.N. Lukyanenko, A.S. Sinitsyn, D.S. Fedorov, K.S Shcherban, *Resonant set-up patent RU 2 348 022 C1* (2009)
12. M. Nemirovsky, *Fatigue test set-up patent RU 2 714 957 C1* (2020)
13. A.B. Kudryashov, D.S. Fedorov, K.C. Shcherban, Aviation industry **4**, 1-10 (2010)
14. R.H. MacNeal, *The NASTRAN Theoretical Manual* (1972)